AGU PUBLICATIONS

Water Resources Research

RESEARCH ARTICLE
10.1002/2016WR019305

**Key Points:**
- Frequency of very wet and dry days has been increasing in the western Amazon in recent decades
- Changes in the frequency of very wet and dry days are related to oceanic and atmospheric variability in the Tropical Pacific and Atlantic
- The vegetation of the western Amazon appears to be more sensitive to the frequency of dry days than to the dry-season rainfall amount

**Supporting Information:**
- Supporting Information S1

**Correspondence to:**
J. C. Espinoza,
jhan-carlo.espinoza@igp.gob.pe

**Citation:**
Espinoza, J. C., H. Segura, J. Ronchail, G. Drapeau, and O. Gutierrez-Cori (2016), Evolution of wet-day and dry-day frequency in the western Amazon basin: Relationship with atmospheric circulation and impacts on vegetation, *Water Resour. Res.*, *52*, doi:10.1002/2016WR019305.

Received 4 JUN 2016
Accepted 17 OCT 2016
Accepted article online 22 OCT 2016



# Evolution of wet-day and dry-day frequency in the western Amazon basin: Relationship with atmospheric circulation and impacts on vegetation

**Jhan Carlo Espinoza[1], Hans Segura[1], Josyane Ronchail[2], Guillaume Drapeau[3], and Omar Gutierrez-Cori[1,4]**

[1]Subdirección de Ciencias de la Atmósfera e Hidrósfera, Instituto Geofísico del Perú, Lima, Peru, [2]Université Paris Diderot, Sorbonne Paris Cité, UMR Locean (Sorbonne Universités-UPMC, CNRS, IRD, MNHN), Paris, France, [3]Université Paris Diderot, Sorbonne Paris Cité, UMR PRODIG, Paris, France, [4]Universidad Agraria La Molina, Lima, Peru

**Abstract** This paper documents the spatiotemporal evolution of wet-day and dry-day frequency (WDF and DDF) in the western Amazon, its relationships with oceanic and atmospheric variability and possible impact on vegetation. WDF and DDF changed significantly during the 1980–2009 period ($p < 0.05$). An increase in WDF is observed after 1995 over the northern part of the western Amazon (Marañón basin). The average annual value of WDF changed from 22 days/yr before 1995 to 34 days after that date (+55% after 1995). In contrast, DDF increased significantly over the central and southern part of this region (Ucayali basin) after 1986. Average annual DDF was 16.2 days before 1986 and 23.8 days afterward (+47% after 1986). Interannual variability in WDF appears to be modulated by changes in Pacific SST and the Walker cell during the November–March season. This mechanism enhances convective activity over the northern part of the western Amazon. The increase in DDF is related to warming of the North Tropical Atlantic SST, which produces changes in the Hadley cell and subsidence over the central and the southern western Amazon. More intense seasonal hydrological extremes in the western Amazon therefore appear to be related to changes in WDF and DDF that occurred in 1995 and 1986, respectively. During the 2001–2009 period, an index of vegetation condition (NDVI) appears negatively correlated with DDF ($r = -0.95$; $p < 0.0001$). This suggests that vegetation in the western Amazon is mainly water limited, rather than light limited and indicates that the vegetation is highly sensitive to concentration of rainfall.

## 1. Introduction

In recent years, several scientific studies have indicated that the Amazon basin has been experiencing a biophysical transition [e.g., *Davidson et al.*, 2012; *Brienen et al.*, 2015; *Nobre et al.*, 2016]. This ongoing change in Amazonian environments has frequently been associated with large-scale climatic variability and many extreme hydrological events have been reported in recent years [e.g., *Callède et al.*, 2004; *Espinoza et al.*, 2009a, 2009b; *Gloor et al.*, 2013; *Marengo and Espinoza*, 2015], including exceptional floods and droughts [e.g., *Marengo et al.*, 2008, 2013; *Zeng et al.*, 2008; *Chen et al.*, 2010; *Espinoza et al.*, 2011, 2013, 2014; *Satyamurty et al.*, 2013a]. In examining droughts, several studies have reported an increase in the length of the dry season, particularly in the southern Amazon since the 1980s, with the wet season beginning later and ending earlier [*Salazar et al.*, 2007; *Phillips et al.*, 2009; *Marengo et al.*, 2011; *Saatchi et al.*, 2012; *Fu et al.*, 2013; *Yin et al.*, 2014; *Arias et al.*, 2015; *Debortoli et al.*, 2015; *Zou et al.*, 2015].

The impacts of drought on Amazonian rainforest vegetation have been analyzed in previous studies, with contradictory results [*Bonal et al.*, 2016] that are related to the debate about whether Amazonian forests are water-limited or light-limited ecosystems. A first group of studies, based on optical remote-sensing and eddy flux data, found that photosynthesis increases in the Amazon rainforest during the dry season in both normal and extreme years [*Huete et al.*, 2006; *Myneni et al.*, 2007; *Saleska et al.*, 2007]. This is consistent with the leaf flush observed during the dry season and it is explained by the peak of solar irradiation under these cloud-free, light-rich conditions. This view holds that water resources are sufficient during the year and therefore are not a limiting factor for rainforest productivity.

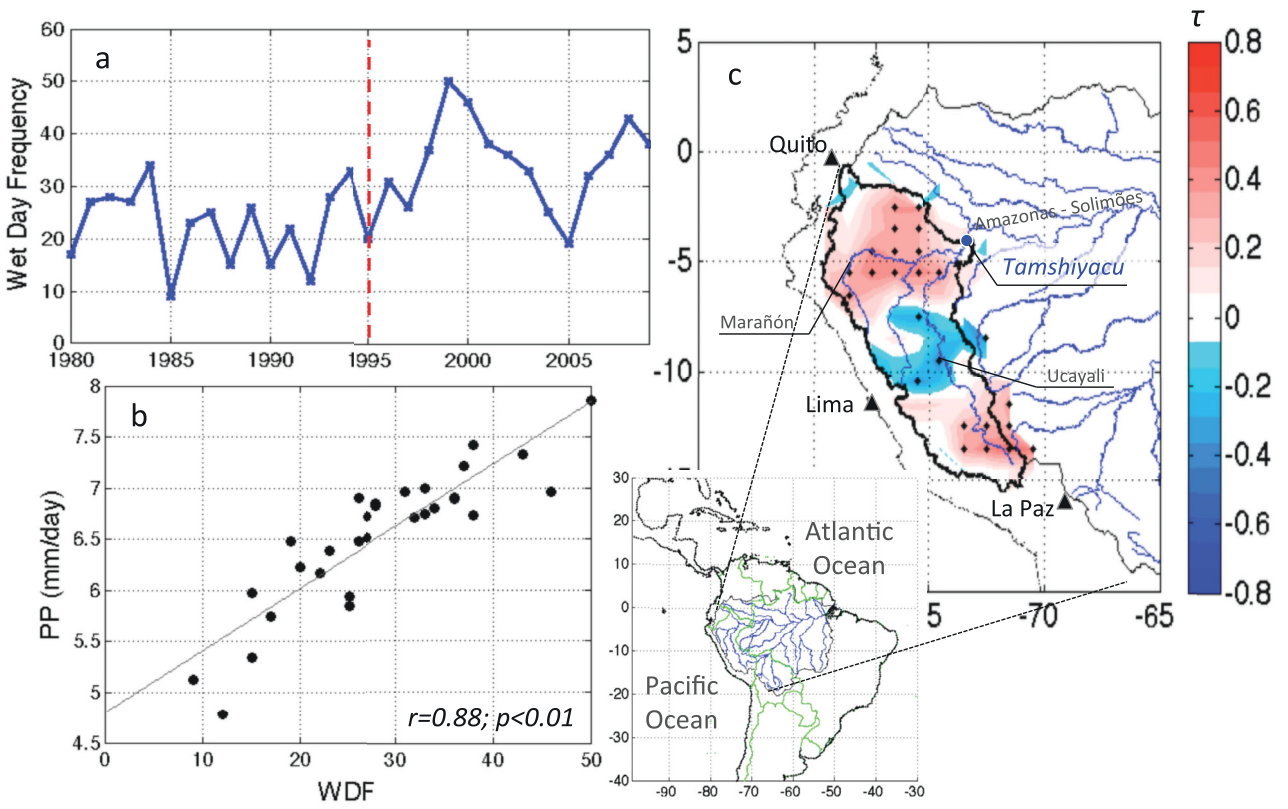


**Figure 1.** (a) 1980–2009 temporal evolution of the annual wet-day frequency (WDF) in the Peruvian-Ecuadorian Amazon basin upstream of Tamshiyacu station. The vertical red line indicates a significant break in 1995 according to Pettitt test at $p < 0.05$. (b) Scatterplot between the annual wet-day frequency (WDF) and mean rainfall (mm/d) during the November–March season (1980–2009). The coefficient of correlation and the *p*-value are indicated. (c) Spatial distribution of Kendall coefficient values ($\tau$) resulting from trend test on gridded WDF values. The $p < 0.05$ values are indicated with dark dots. The location of the Amazon basin in South America, and of the main cities and rivers mentioned in the text are indicated.

But this paradigm of a light-limited rainforest was contradicted by in situ observations of increased tree mortality during the droughts [*Phillips et al.*, 2009]. It has also been challenged by several studies that have questioned the reproducibility of the analyses, the quality of the data or artifacts inherent to the remote-sensing data [*Samanta et al.*, 2010; *Atkinson et al.*, 2011; *Morton et al.*, 2014]. Other studies have described a water-limited rainforest, with widespread declines in greenness [*Xu et al.*, 2011] or decreasing gross primary production [*Lee et al.*, 2013] during droughts, indicating a loss of photosynthetic capacity due to water stress. Nevertheless, a recent study by *Maeda et al.* [2014] reports a greening of vegetation during the dry season even with the correction of data and artifacts. Taking these contradictory results into account, *Hilker et al.* [2014] distinguish between light-limited rainforests, which green up during the dry season, and where deep-rooted trees can access groundwater, and water-limited rainforests, which brown down during droughts. The most severe droughts (2005, 2010), however, showed that large-scale die-off of vegetation can affect both types of ecosystems.

Prolonged fire seasons are also observed during extreme droughts [*Aragão et al.*, 2007; *Fernandes et al.*, 2011; *Brando et al.*, 2014], as a delayed ending of the dry season has been related to an increase in the number of fires in the southern Amazon [*Fu et al.*, 2013]. Higher rates of tree mortality and increased forest flammability appear particularly related to prolonged periods of a critically low level of soil moisture [*Nepstad et al.*, 2004]. This confirms the relevance of monitoring the frequency of dry and wet days rather than just the amount of seasonal precipitation.

The Peruvian-Ecuadorian Amazon basin, upstream from the Tamshiyacu hydrological station on the Amazon River in Peru (Figure 1), covers a large drainage area of about 750,000 km$^2$, including most of the Andean-Amazon transition region. The long-term mean discharge at Tamshiyacu is estimated at 32,000 m$^3$/s (about twice the mean discharge of the Mississippi), which corresponds to 16% of the Amazon discharge at

the estuary [*Espinoza et al*., 2009b]. Total annual rainfall over this basin is estimated at 1750 mm/yr [*Espinoza et al*., 2011]; in the Andean-Amazon transition region, however, there are "hotspots" where annual rainfall exceeds 5000 mm/yr locally [*Espinoza et al*., 2009a, 2015].

In the western Amazon, significant changes have also been identified in hydroclimatic conditions. Analysis of mean annual rainfall and discharge at the Tamshiyacu station shows negative trends since the 1970s [*Espinoza et al*., 2011; *Lavado et al*., 2013], with a statistical break in 1986 and a subsequent decrease in minimum monthly runoff [*Espinoza et al*., 2009b]. Previous studies have found a relationship between seasonal hydrological extremes (floods and droughts) and climate variability, including anomalies in sea surface temperature (SST) in the Equatorial Pacific and Tropical Atlantic oceans. Extreme rainfall and resulting flooding in the western Amazon have been associated with cool conditions in the Equatorial Pacific Ocean, as seen in 1989, 1999, and 2012 (i.e., La Niña events) [*Ronchail et al*., 2006; *Marengo et al*., 2013; *Espinoza et al*., 2012a,; *Lavado et al*., 2013]. These studies show an increase in water vapor flux from the North Tropical Atlantic to the northwestern Amazon basin during La Niña years. However, previous studies have also shown that warm conditions in the Equatorial Pacific Ocean (i.e., El Niño events) produce atmospheric teleconnections that result in rainfall deficits and, consequently, extreme droughts in the western Amazon, as occurred in 1998 [*Espinoza et al*., 2011; *Lavado and Espinoza*, 2014]. During El Niño years, there is weaker moisture advection from the North Tropical Atlantic to the western Amazon and higher water vapor transport from the Amazon basin toward the La Plata Basin. Warm conditions in the North Tropical Atlantic have been associated with rainfall deficits that explain the recent extreme droughts in the western Amazon in 1995, 2005, and 2010 [*Marengo et al*., 2008, 2011; *Yoon and Zeng*, 2010; *Espinoza et al*., 2011]. These studies documented reduced trade winds and weaker moisture advection from the Atlantic toward Amazonia during the austral autumn and winter during warm episodes in the North Tropical Atlantic. For a complete description of the causes of extreme seasonal hydrological events in Amazonia, see *Marengo and Espinoza* [2015].

Future climate scenarios based on general circulation models show a possible increase of dry-day frequency in Amazonia [*Polade et al*., 2014] and an intensification of extreme hydrological events such as seasonal floods and droughts [e.g., *Guimberteau et al*., 2013; *Boisier et al*., 2015; *Sorribas et al*., 2016]. *Polade et al*. [2014] suggest that a decrease in annual rainfall in the Amazon basin could be dominated by an increase in the number of dry days. This increase could amount to 30 more dry days per year by the end of the 21st Century.

Better monitoring and understanding of wet-day and dry-day frequency in Amazonia become essential for assessing the sustainability of Amazonian ecosystems. Ecological services provided by the Amazonian rainforest strongly depend on the availability of water during the dry season, as either precipitation or stored soil moisture. These factors also affect rural livelihoods, because fishing and annual floodplain agriculture are impacted by extreme rainfall events and rapid changes in river stage [*Coomes et al*., 2016]. Analysis of the structure of rainfall intensity on a daily time scale and of the evolution of wet-day and dry-day frequency in the western Amazon can provide new information for assessing the possible impacts of climate on vegetation (e.g., increased water stress because of a longer dry season), on the frequency of hydrological extremes (floods and droughts) and on water resources in this region. This paper analyzes the spatiotemporal evolution of wet-day and dry-day frequency in the Peruvian-Ecuadorian Amazon basin and their relationship to oceanic and atmospheric variability. This study especially aims to provide physical explanations of changes in the structure of the wet and dry seasons and their possible impacts on vegetation.

## 2. Hydroclimate Data Sets and Methods

### 2.1. Gridded HYBAM Observed Precipitation (HOP) Data

HYBAM Observed Precipitation (HOP) data is a gridded ($1^\circ \times 1^\circ$ horizontal resolution) data set derived from 752 meteorological stations in five countries. Data are collected by the national institutions in charge of hydrometeorological monitoring: the National Water Agency (ANA) in Brazil, the National Meteorology and Hydrology Service (SENAMHI) in Peru and Bolivia, the National Meteorology and Hydrology Institute (INAMHI) in Ecuador and the Hydrology, Meteorology, and Environmental Studies Institute (IDEAM) in Colombia. The HOP data set is available from 1980 to 2009 on a daily time step [*Guimberteau et al*., 2012]. In the Peruvian-Ecuadorian Amazon basin, delimited by the Tamshiyacu hydrological station, HOP is

computed from 234 meteorological stations from INAMHI and SENAMHI of Peru [*Espinoza et al*., 2011]. For more details about quality control of the rainfall data and geostatistical interpolation of rainfall observations, see *Guimberteau et al*. [2012]. Gridded HOP daily data are freely available in NetCDF format at www.ore-hybam.org.

### 2.2. Ocean and Atmospheric Data Sets

Oceanic data are analyzed using the global monthly SST data available at 2° resolution from NOAA-CPC [*Reynolds and Smith*, 1994]. Atmospheric circulation is analyzed using horizontal and vertical winds and specific humidity data at 2.5° resolution from the NCEP-NCAR reanalysis [*Kalnay et al*., 1996]. The accuracy of NCEP-NCAR reanalysis, particularly of rainfall variability and extreme hydroclimatic events, has already been tested over this region [e.g., *Satyamurty et al*., 2013b; *Yoon and Zeng*, 2010; *Espinoza et al*., 2011, 2013]. Wind circulation and specific humidity are analyzed from 1000 to 100 hPa and from 1000 to 300 hPa, respectively. Vertically integrated water vapor flux and its divergence are derived from specific humidity and horizontal wind using pressure levels of 1000, 925, 850, 700, 600, 500, 400, and 300 hPa [*Peixoto and Oort*, 1992]. The difference in potential temperature between 700 and 400 hPa is also computed to evaluate atmospheric stability. Finally, we also use daily interpolated Outgoing Longwave Radiation (OLR) data from NCAR/NOAA [*Liebmann and Smith*, 1996]. OLR data are generally considered a proxy for deep convection in tropical regions [e.g., *Liebmann et al*., 1999; *Jones et al*., 2004; *Villacís et al*., 2008; *Espinoza et al*., 2012b].

### 2.3. Vegetation Indices Over the Western Amazon

We use the normalized difference vegetation index (NDVI) computed from the MOD13C1 product provided by the Moderate Resolution Imaging Spectroradiometer (MODIS) sensor, as an indicator of vegetation greenness. NDVI validations over the Amazon basin can be found in previous papers [e.g., *Huete et al*., 2002; *Xu et al*., 2011; *Hilker et al*., 2015]. MOD13C1 (0.05° resolution) are computed from the spatial average of the 16 day MOD13A2 product, available at 1 km spatial resolution [*Solano et al*., 2010]. To improve the quality of the NDVI data, we compute monthly composites from the 16 day data by selecting the best pixels from each month, considering atmospheric conditions, using the maximum value composition (MVC) technique [*Huete et al*., 2002]. This provides a data set with a lower temporal resolution, but with higher quality at a monthly time step [*Holben*, 1986]. The Zavitsky-Golay temporal filter is applied to each pixel [*Chen et al*., 2004] to reduce atmospheric noise and distortion. Finally, mean values for the August–October season are computed for each pixel to analyze interannual variability of vegetation conditions over the Tamshiyacu basin.

### 2.4. Statistical Analysis in the Time Series

The relationship between the frequency of wet and dry days and oceanic/atmospheric variables and NDVI values are investigated using linear regression analysis by means of the parametric Pearson coefficient (r). Statistical breaks in the time series are evaluated using the Pettitt method [*Pettitt*, 1979], a nonparametric test based on changes in the average and the range of the series. The Pettitt test is considered one of the most complete tests for identifying changes in hydroclimate time series [*Zbigniew*, 2004; *Espinoza et al*., 2009b]. To identify temporal trends in time series, we use the rank-based nonparametric Kendall test [*Kendall*, 1975]. The significance of statistical tests is evaluated at 90% ($p < 0.1$), 95% ($p < 0.05$), and 99% ($p < 0.01$).

## 3. Evolution of Wet-Day and Dry-Day Frequency in the Western Amazon

In this section, we analyze the spatiotemporal evolution of wet-day frequency (WDF) and dry-day frequency (DDF). Over the Tamshiyacu basin, annual WDF is defined as the frequency of days with rainfall greater than 10 mm, which is about twice the mean annual rainfall in the Tamshiyacu basin (estimated at 4.8 mm/d) [*Espinoza et al*., 2011]. Analysis of each month's contribution to annual WDF shows an annual cycle from September to August, which appears dominant in both the southern and northern parts of the Tamshiyacu basin (supporting information Figure S1a). Annual WDF is therefore computed from September (n-1) to August (n). Annual DDF is defined as the frequency of days with rainfall of less than 1 mm. Analysis of each month's contribution to annual DDF shows an annual cycle from January to December, with peak values from April to September in the South and July to September in the North. The lowest values are observed

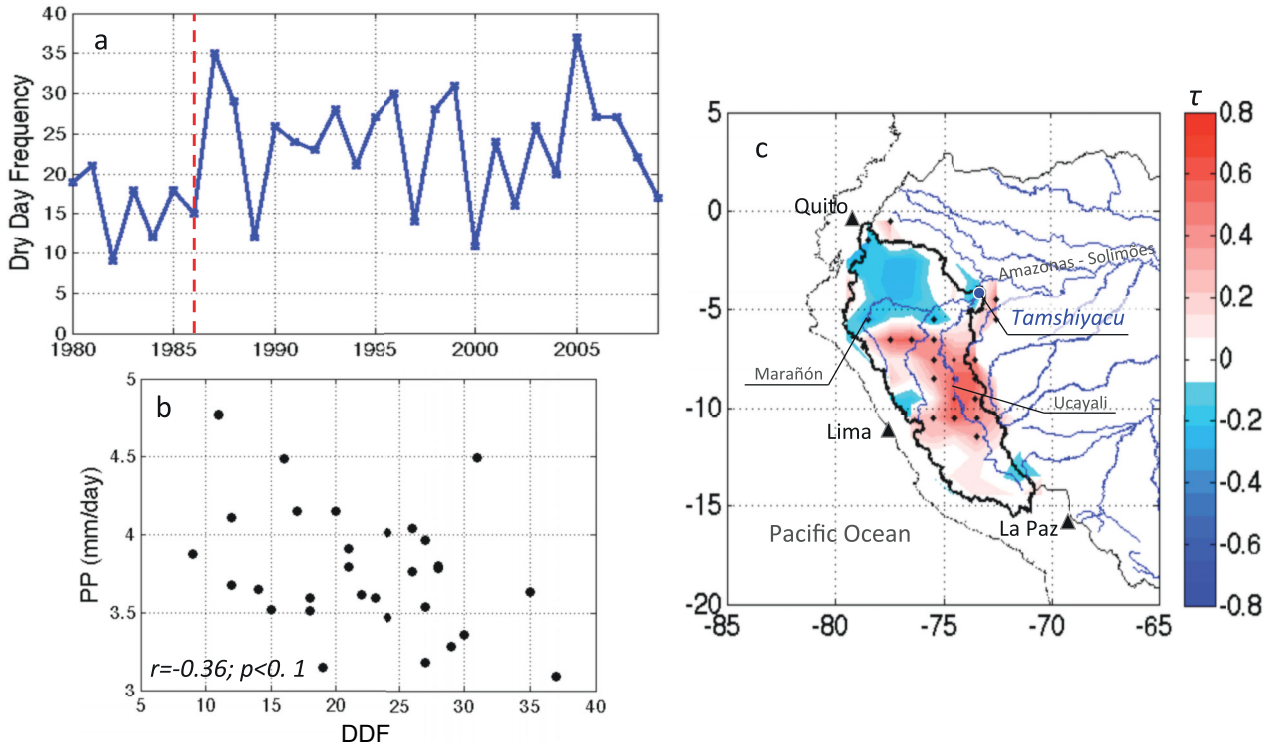


**Figure 2.** (a) 1980–2009 temporal evolution of the annual dry-day frequency (DDF) in the Peruvian-Ecuadorian Amazon basin upstream of the Tamshiyacu station. The vertical red line indicates a significant break in 1986 according to Pettitt test at $p < 0.05$. (b) Scatterplot between the annual dry-day frequency (DDF) and mean rainfall (mm/d) during the April–August season (1980–2009). The coefficient of correlation, and *p*-value are indicated. (c) Spatial distribution of Kendall coefficient values ($p < 0.05$ are indicated with a dark dots) resulting from trend test on gridded DDF values. The main cities and rivers mentioned in the text are indicated.

from December to March in both the northern and southern Tamshiyacu basin (supporting information Figure S1b). Annual DDF is therefore computed from January (n) to December (n).

A basin-averaged analysis shows a significant increase ($p < 0.05$) in WDF over the Tamshiyacu basin (Figure 1a). The Pettit test detects a break in the WDF time series in 1995, with an average of 22 wet days per year before 1995 and 34 wet days per year afterward. This change corresponds to an increase of 55% in WDF. The highest WDF value is observed in 1999, when an extreme flood, associated with a La Niña event, was reported in this basin [*Espinoza et al*., 2013; *Marengo and Espinoza*, 2015]. Some low WDF values correspond to dry years in the western Amazon, such as 1992 and 2005. It is noteworthy that WDF values are highly correlated with total rainfall for the rainy season (November–March), averaged over the Tamshiyacu basin (Figure 1b). Variability of annual WDF therefore explains about 77% of rainfall evolution during the wet period. The increasing WDF after 1995 is also consistent with the low-frequency rainfall variability during the austral summer reported in the western Amazon by *Grimm and Saboia* [2015]. This indicates that the high frequency of extreme seasonal flooding in the Tamshiyacu basin in recent decades might be a response to the increase in WDF after 1995 (extreme seasonal floods in 1999; 2009, 2012). Figure 1c provides a spatial observation of the WDF trend using the Kendall test. It shows a significant increase in WDF over the northern Tamshiyacu basin (lower Marañón basin and left bank of the Amazon River) and in the extreme South (upper Ucayali basin; Apurimac and Urubamba basins). Some regions in the lower Ucayali basin, meanwhile, show a downward trend in WDF (around 10°S–7°S; Figure 1c). The increase in WDF in the northern Tamshiyacu basin has relevant hydrological implications because this region is among the rainiest areas in the Amazon basin [e.g., *Espinoza et al*., 2009a].

Analysis of the evolution of DDF over the Tamshiyacu basin using the Pettitt test shows a break in 1986 (Figure 2a). DDF increases from an average of 16.2 days/yr before 1986 to 23.8 days/yr after 1986, a 47% increase. The break in 1986 and the DDF increase afterward are consistent with the significant change in the amount of runoff and rainfall during the low-stage period at the Tamshiyacu station detected in 1986

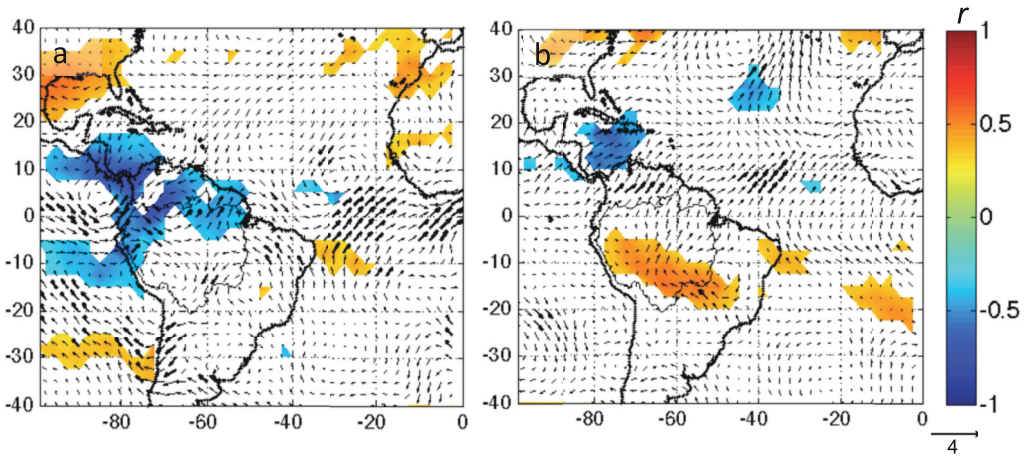


**Figure 3.** (a) 1980–2009 correlation between WDF in the Tamshiyacu basin versus November–March Outgoing Longwave Radiation (OLR; colors, only r-values significant at $p < 0.1$ are plotted) and vertically integrated water vapor flux (vectors, r-values significant at $p < 0.1$ are represented as bold vectors). (b) Similar to Figure 3a but considering DDF and atmospheric variables for the April–August season.

by *Espinoza et al*. [2009b]. According to this study, runoff during the low-water period at the Tamshiyacu station decreases by 18% after 1986. *Espinoza et al*. [2011] also reported a significant decrease in rainfall in the Tamshiyacu basin for the 1970–2010 period; this was particularly intense during the dry season. Although annual DDF is highly dependent on the April–August season (supporting information Figure S1b) and some years with high DDF are extremely dry, such as 2005 (Figure 2b), basin-averaged rainfall during the dry season (April–August) appears poorly correlated with DDF in the Tamshiyacu basin ($r = -0.36$, $p < 0.1$; Figure 2b). This is probably related to the spatial distribution of rainfall over the basin. Indeed, rainfall during April–August is higher over the northern part of the basin and lower over the southern region. Figure 2c shows a spatial overview of the DDF trend over the Tamshiyacu basin. There is a significant increase in DDF ($p < 0.05$) in the central and southern Tamshiyacu basin (Ucayali River). Runoff of the Ucayali River at the Requena station has also decreased since the 1990s [*Espinoza et al*., 2009b].

These results suggest that the frequency of wet and dry days in the western Amazon has changed significantly during 1980–2009. WDF increased after 1995, particularly over the northern Tamshiyacu basin (Marañón basin), while DDF increased significantly over the central and southern part of the basin (Ucayali basin), particularly after 1986. This pattern of change is consistent with the intensification of the hydrological cycle detected in the Amazon basin in recent decades [e.g., *Callède et al*., 2004; *Espinoza et al*., 2011, 2013; *Gloor et al*., 2013; *Marengo and Espinoza*, 2015].

## 4. Oceanic and Atmospheric Features Associated With Changes in Rainfall Intensity

In this section, we explore the relationships between the evolution of WDF and DDF and oceanic and atmospheric variables during the wet period (November–March) and dry period (April–August). Interannual WDF variability appears positively correlated with a northerly water vapor flux and negatively correlated with OLR over the northern part of the Tamshiyacu basin (north of 10°S; Figure 3a). This suggests that the increase in WDF can be related to a northerly flow from the Caribbean Sea and Equatorial Pacific Ocean that provide humidity to the northwestern Amazon. These mechanisms produce enhanced convective activity over the northern part of the Tamshiyacu basin (Marañón basin; Figure 3a), the region where a significant increase in WDF has been observed (Figure 1c).

DDF is significantly correlated with a southerly water vapor flux in the North Tropical Atlantic Ocean and over the extreme north of South America during the dry period (April–August; Figure 3b). This circulation produces a weaker water vapor flux toward the southwestern Amazon, where convective activity is reduced, as shown by the positive correlation between DDF and OLR (red color in Figure 3b). In contrast, water vapor remains over the Caribbean Sea, producing convective activity there (from 10°N to 20°N; blue

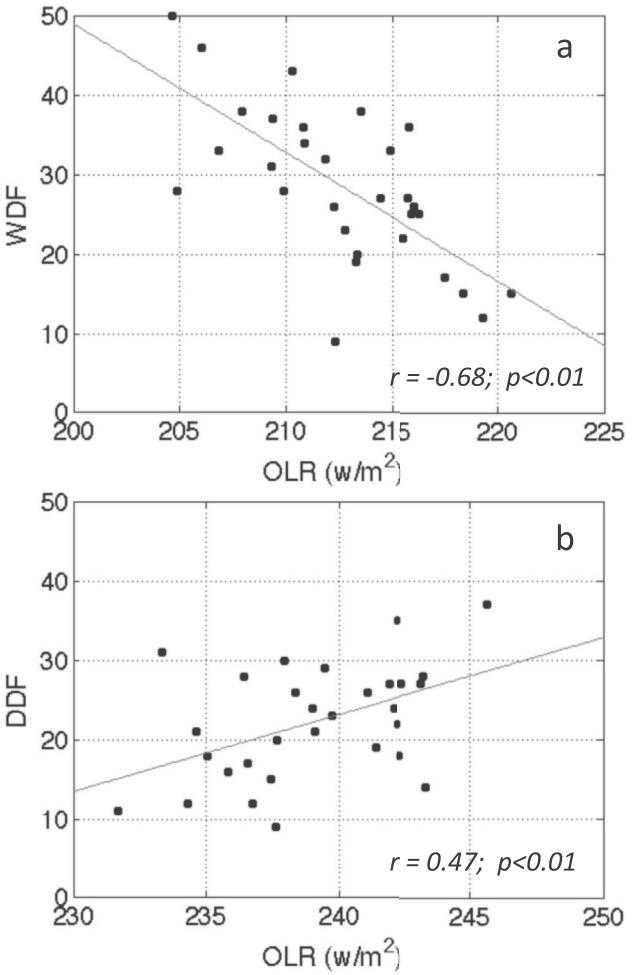


**Figure 4.** (a) Scatterplot of mean November–March OLR in the northern Tamshiyacu basin (0°S–10°S and 80°W–70°W) versus WDF over the Tamshiyacu basin for the 1980–2009 period. (b) Scatterplot of mean April–August OLR in the southern Tamshiyacu basin (5°S–12.5°S and 87.5°W–70°W) versus DDF over the Tamshiyacu basin for the 1980–2009 period. Regression lines, coefficient of correlations, and *p*-values are indicated.

color in Figure 3b). The positive correlation between DDF and OLR is predominant over the southern Tamshiyacu basin, where a positive trend in DDF is observed (Figure 2c).

Regionally averaged OLR values over the northern Tamshiyacu basin (0°S–10°S and 80°W–70°W region) during November–March appear significantly correlated with WDF ($r = -0.68$; $p < 0.01$; Figure 4a). This means that years when there is intense convective activity in the northern Tamshiyacu basin during the November–March season are also years with high WDF. Regionally averaged OLR in the northern Tamshiyacu basin also shows a significant decrease after 1995 ($p < 0.05$; not shown), which is consistent with the increase in WDF and mean rainfall during the wet season over this region after 1995 (Figures 1a and 1b). Similarly, regionally averaged OLR over the southern Tamshiyacu basin (5°S–12.5°S and 77.5°W–70°W region) during the April–August season appears significantly correlated with DDF ($r = 0.47$; $p < 0.01$; Figure 4b), which suggests that years with weak convective activity are associated with high DDF. While the correlations with regional OLR are significant ($p < 0.01$) for both the WDF and DDF time series, it is remarkable that the correlation between WDF and OLR is higher during the wet period (November–March).

The evolution of WDF and DDF is also related to sea surface temperature (SST; Figure 5). November–March SST shows a significant correlation with WDF in the extreme western part of the Tropical Pacific Ocean, where a positive correlation is observed, and in the central Equatorial/North Tropical Pacific Ocean (around 150°W), where a negative correlation is observed (Figure 5a). This result is consistent with the increase in daily rainfall in the northwestern Amazon during La Niña years, as compared to El Niño years [*Ropelewski and Bell*, 2008], and with extreme floods in the western Amazon, which are frequently related to La Niña events [*Espinoza et al*., 2012a, 2013; *Lavado et al*., 2013; *Marengo and Espinoza*, 2015]. The authors have documented an intensification of water vapor flux from the North Tropical Atlantic over the northern Amazon basin and an increase in rainfall amounts over this region during La Niña years.

DDF variability is positively correlated with SST during the dry season (April–August) over the North Tropical Atlantic Ocean, the Caribbean Sea and the Indian Ocean (Figure 5b). Positive correlation between DDF and North Tropical Atlantic and Caribbean Sea SST is consistent with previous studies that documented negative rainfall anomalies over the southwestern Amazon, such as the extreme droughts of 2005 and 2010, during warm episodes in the North Tropical Atlantic [*Marengo et al*., 2008, 2011; *Yoon and Zeng*, 2010; *Espinoza et al*., 2011; *Marengo and Espinoza*, 2015]. When the North Tropical Atlantic is warmer than usual, water vapor flux from the Atlantic Ocean and Caribbean Sea toward the Amazon basin is reduced.

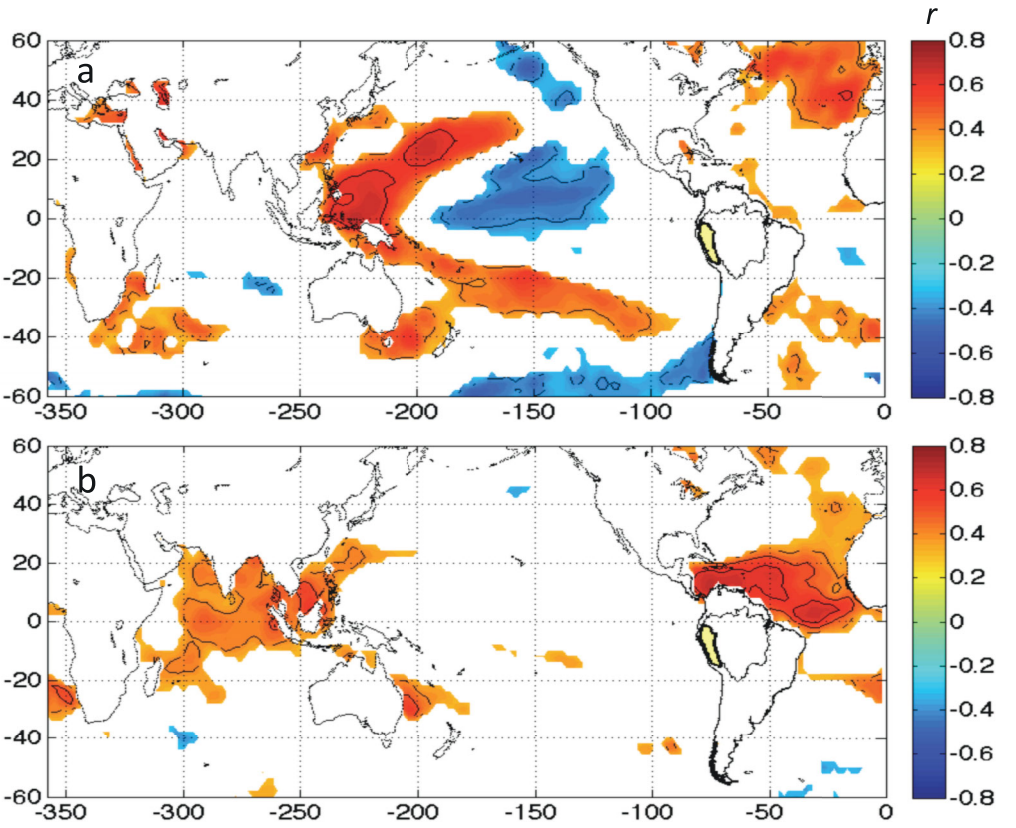


**Figure 5.** (a) Correlation between November–March SST versus WDF in the Tamshiyacu basin (1980–2009). (b) Correlation between April and August SST versus DDF in the Tamshiyacu basin (1980–2009). Only values with $p < 0.05$ are plotted (contours indicate significance at $p < 0.01$).

The particular influence of the Pacific and Atlantic oceans on WDF and DDF, respectively, is consistent with teleconnection patterns previously identified between these oceans and rainfall in the Amazon. During the December–April season, the Equatorial Pacific Ocean plays a major role in modulating rainfall over the western Amazon [*Yoon and Zeng*, 2010; *Ropelewski and Bell*, 2008]. During this season, the Atlantic Ocean does not show a significant influence on rainfall in the Amazon. During the July–October season, however, SST over the North Tropical Atlantic region is highly correlated with rainfall in the Amazon, while correlation with the Pacific Ocean disappears [*Espinoza et al*., 2009b; *Yoon and Zeng*, 2010]. Because WDF and DDF mainly occur during the austral summer and austral winter, respectively (supporting information Figure S1), WDF is assumed to be modulated mainly by Equatorial Pacific SST while DDF is modulated mainly by North Tropical Atlantic SST.

Our results show a statistical association between global SST and WDF/DDF in the Tamshiyacu basin, which suggests a remote influence of SST by atmospheric teleconnections. To explore these atmospheric mechanisms, we analyze the correlation between large-scale atmospheric circulation and WDF/DDF variability (Figure 6). Figure 6a shows the correlation between WDF and the November–March atmospheric circulation in a cross section (longitude versus pressure level) over the Equatorial Pacific (10°N–10°S). High values of WDF are associated with enhanced wind ascendance and higher-than-usual specific humidity in the western Equatorial Pacific, subsidence and weak specific humidity in the central Equatorial Pacific, and enhanced ascendance and higher specific humidity over Equatorial South America (particularly east of the Andes, in a region corresponding to the northern Tamshiyacu basin; Figure 6a). In the Pacific Ocean, the region characterized by wind ascendance/subsidence in Figure 6a (positively/negatively correlated with WDF) is also characterized by warm/cool SST (positively/negatively correlated with WDF in Figure 5a). Figures 5a and 6a therefore suggest that the interannual variability of WDF in the western Amazon is modulated by modifications in the Pacific Walker cell, which enhance convective activity over the northern Tamshiyacu basin.

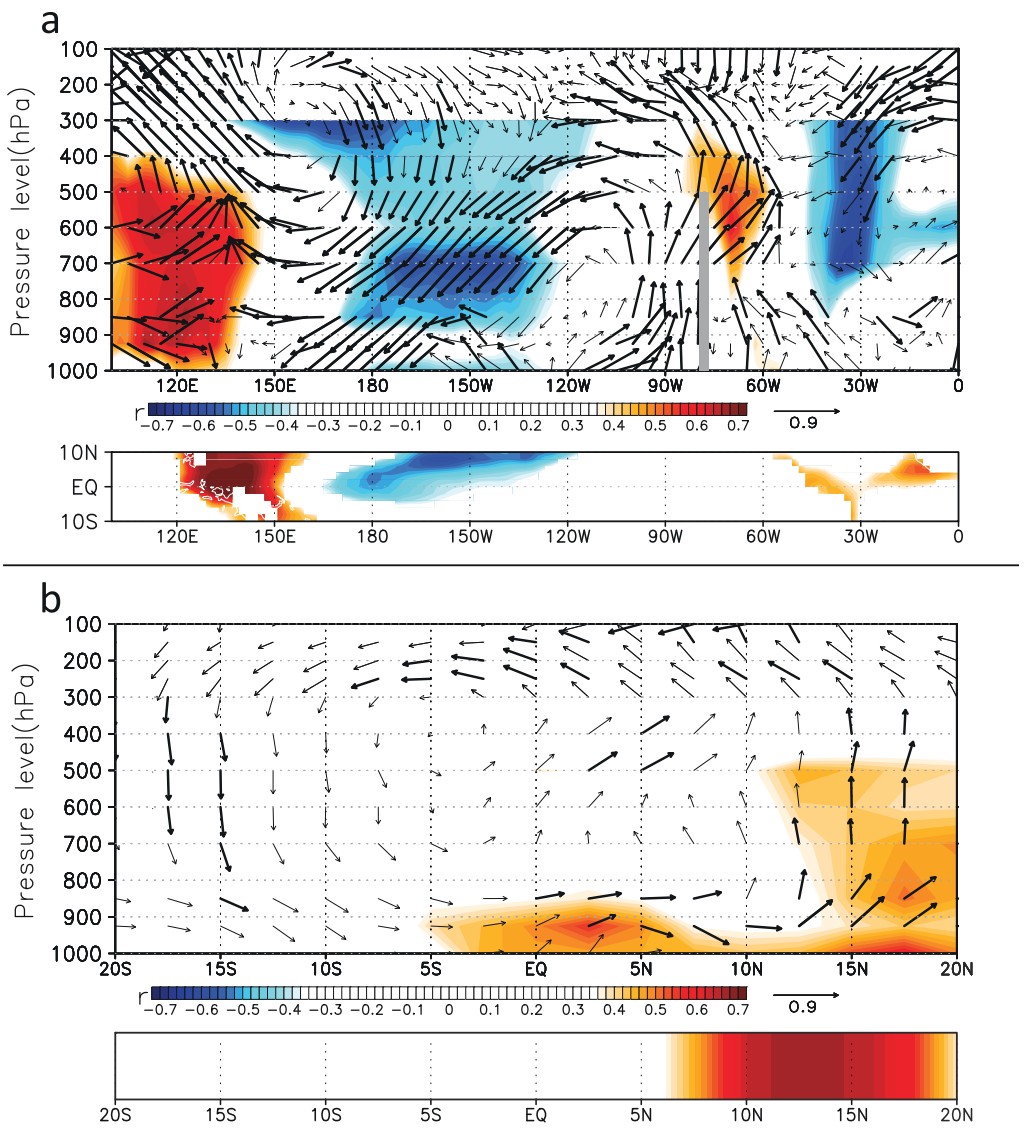


**Figure 6.** (a) 1980–2009 correlation in a cross section (longitude versus pressure level) between WDF in the Tamshiyacu basin versus November–March specific humidity (colors) and total winds (vectors). Total winds and specific humidity are averaged for the 10°N and 10°S region. The correlation between November–March SST versus WDF is shown at the bottom (as Figure 5a, but considering 10°N–10°S region). (b) 1980–2009 correlation in a cross section (latitude versus pressure level) between DDF in the Tamshiyacu basin versus April–August specific humidity (colors) and total winds (vectors). Total winds and specific humidity are averaged for the 80°W and 70°W region. The correlation between April–August SST versus DDF is shown at the bottom (as Figure 5b, but considering 10°N–10°S region). In Figures 6a and 6b, only colors with r-values significant at $p < 0.05$ are plotted and bold vectors correspond to r-values significant at $p < 0.05$.

Figure 6b shows a correlation between DDF and April–August wind circulation in a cross section (latitude versus pressure) averaged over the 70°W–80°W region. During years of high DDF in the Tamshiyacu basin, southerly wind anomalies near the surface predominate over the western Amazon and northern South America, while enhanced wind ascendance is observed over the Caribbean Sea (Figure 6b). Specific humidity in the northern part of the section (north of 5°S) is also positively correlated with DDF. The signal of specific humidity reaches 500 hPa, at about 15°N–20°N, indicating enhanced convective activity over this region. This is consistent with the negative correlation between DDF and OLR in the Caribbean Sea shown in Figure 3b. At higher pressure levels (200–300 hPa), we see northerly winds during years of high DDF, while subsidence predominates in the 10°S–20°S region, in the southern Amazon (Figure 6b). This shows that the interannual DDF variability is modulated by anomalies in the Atlantic Hadley cell. These results are consistent with previous studies, which have documented a decrease in total rainfall in the southern

Amazon during warm episodes in the North Tropical Atlantic because of changes in the Atlantic Hadley cell, including increased wind ascendance and rainfall over the Tropical Atlantic Ocean and increased subsidence and dry conditions over the southern Amazon [e.g., *Yoon and Zeng*, 2010]. Our results complement previous findings by showing that DDF in the western Amazon is also modulated by changes in oceanic and atmospheric conditions related to the Atlantic Hadley cell.

## 5. Ocean-Atmospheric Characteristics Related to the Change of WDF in 1995

As Figures 1a and 2a show, statistical breaks occur in the WDF and DDF time series in 1995 and 1986, respectively. WDF and DDF show higher values after the breaks. The break in 1986 has also been reported for runoff at the Tamshiyacu station during the low-water period [*Espinoza et al*., 2009b] and some studies suggest this is due to the warming of North Tropical Atlantic SST after this date [*Espinoza et al*., 2009b, 2011; *Yoon and Zeng*, 2010; *Marengo et al*., 2011; *Lavado et al*., 2013] as part of decadal variability in Atlantic SST [*Fernandes et al*., 2015]. The increase of WDF in the western Amazon, however, has not been documented in the scientific literature. In this section, we explore oceanic and atmospheric conditions related to the change of WDF in 1995.

In contrast to the 1980–1994 period, the wet seasons of 1995–2009 are characterized by warm SST in the western Tropical Pacific, Indo-Pacific and North Atlantic oceans, and cooler SST in the central Tropical Pacific Ocean (Figure 7a). The spatial structure of change in Pacific Ocean SST seems similar to the correlation between WDF and SST, with warm conditions in regions where positive correlations are observed in Figure 5a. Analyzing large-scale wind circulation and specific humidity in the cross section of the Tropical Pacific Ocean, we observe enhanced subsidence and less specific humidity over the central Tropical Pacific Ocean (Figure 7b). In contrast, increased wind ascendance and specific humidity are observed in the western Tropical Pacific Ocean and east of the Andes (Tamshiyacu basin) after 1995. In addition, the difference in potential temperature between 700 and 400 hPa over the northern Tamshiyacu basin (82.5°W–70° W and 0°S–7°S) for the November–March season is lower during 1995–2009 (−22.7°K) than in 1980–1994 (−23.4°K). The change in the difference in potential temperature is significant at $p < 0.001$ according to a $t$ test. This result indicates an increase in atmospheric instability over the northern Tamshiyacu basin after 1995. Specific humidity is also noticeably higher after 1995 over the Equatorial Atlantic (blue color over 0°W–60°W in Figure 7b), which is probably related to warmer conditions over this oceanic region in recent decades compared to 1980–1994 (Figure 7a). These anomalies in winds, specific humidity and atmospheric stability after 1995 suggest that the increase in WDF over the northern Tamshiyacu basin after this date is probably related to a modification of the Walker cell, which enhances ascendance and convection over the northwestern Amazon (Figure 7b).

## 6. Impacts of DDF on Vegetation Conditions

In this section, we analyze the impact of the increase in DDF over the Tamshiyacu basin on the greenness of vegetation as characterized by NDVI, which is an indicator of photosynthetic capacity. We compute a simple linear regression between the mean August–October NDVI over the Tamshiyacu basin and annual DDF (shown in Figure 2a), using the 2001–2009 common period (Figure 8a). Although this regression is computed for 9 years only, NDVI and DDF over the basin appear significantly correlated ($r = -0.95$; $p < 0.0001$) at an interannual time scale. This correlation is even higher than the correlation between NDVI and rainfall amount during the April–August dry season (Figure 8b; $r = 0.82$; $p < 0.01$). During years characterized by high DDF, NDVI decreases significantly, while high NDVI values correspond to years with low DDF and high rainfall during the dry season (Figures 8a and 8b). For example, high NDVI values are seen during years when floods were reported in the western Amazon (2009 and 2002), while a very low NDVI value was observed during 2005, an extreme drought year. This is consistent with the spread of fires in this region in 2005 [*Fernandes et al*., 2011]. It is also noteworthy that NDVI values during the 2010 (red triangle in Figure 8) and 2005 droughts are very close, 0.69 and 0.70, respectively. The correlation between NDVI and DDF remains significant at $p < 0.01$ when 2005 is removed. This is consistent with previous studies that found a decrease in tree transpiration during extreme droughts [*Bonal et al*., 2016]. A decrease in evapotranspiration during droughts, however, results from two opposite effects: (i) high solar radiation and (ii) decreased water availability in soil. The inverse association between the interannual NDVI and DDF, which is related to

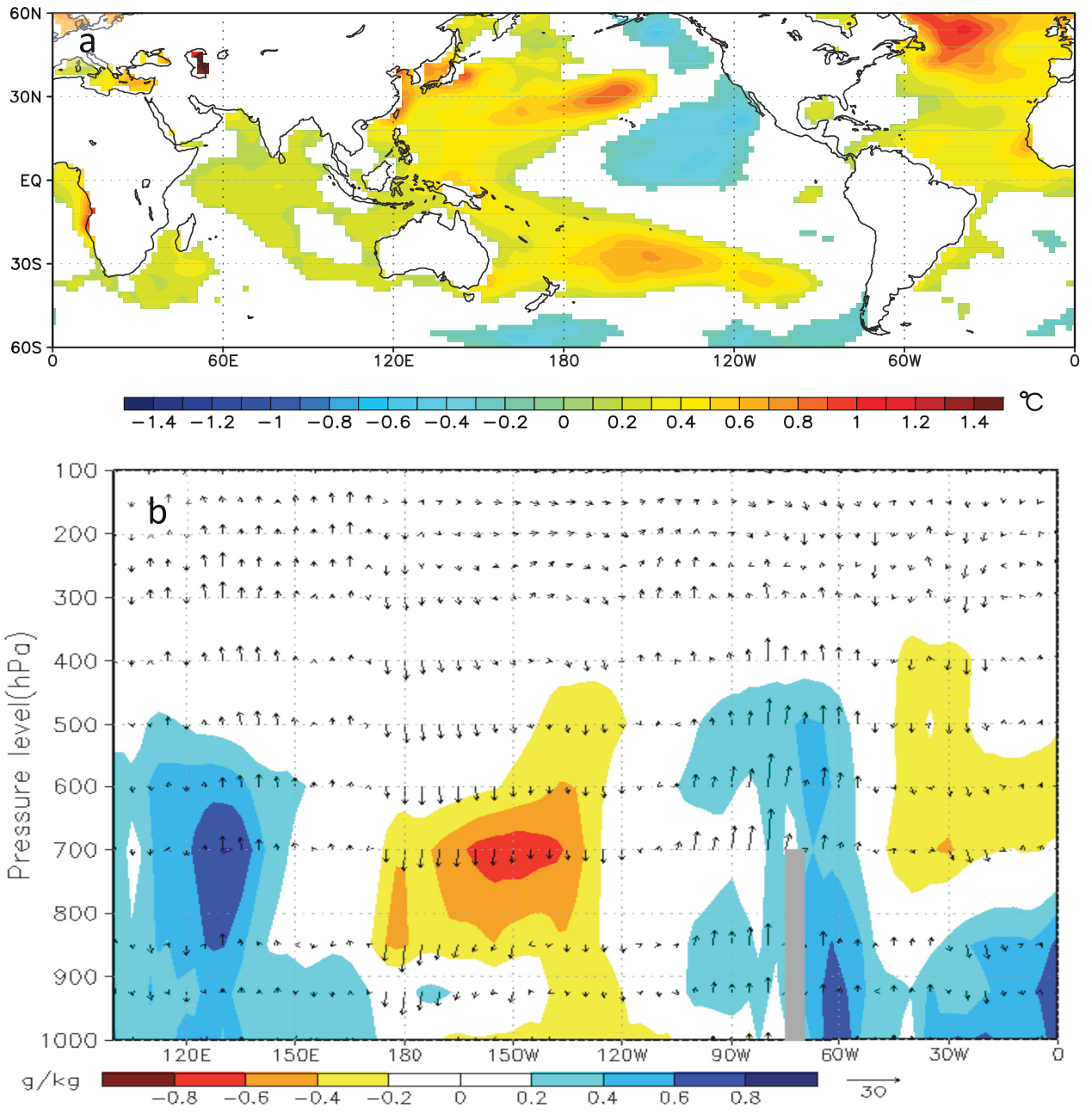


**Figure 7.** (a) 1995–2009 minus 1980–1994 November–March SST. Only differences greater than 2× standard deviation are plotted. (b) 1995–2009 minus 1980–1994 November–March total winds (vectors) and specific humidity (colors) in a cross section (longitude versus pressure level) averaged for the 10°N–10°S region. For specific humidity, only differences greater than ±0.2 g/kg are plotted.

cloud-free atmospheric conditions, suggests that the vegetation in the western Amazon is mainly water limited, rather than light limited. This is consistent with the hypothesis that persistent declines in vegetation greenness occur during extreme droughts [e.g., *Xu et al.*, 2011]. This analysis also indicates that vegetation conditions might be more related to DDF than to the amount of rainfall over the basin, highlighting a strong sensitivity of vegetation to the concentration of rainfall.

Previous studies have documented a widespread decline in greenness of vegetation in the Amazon in the recent past [*Atkinson et al.*, 2011; *Hilker et al.*, 2014]. Because greenness may be related to carbon uptake, this trend is consistent with a long-term increase in biomass mortality and a decrease in carbon accumulation reported in

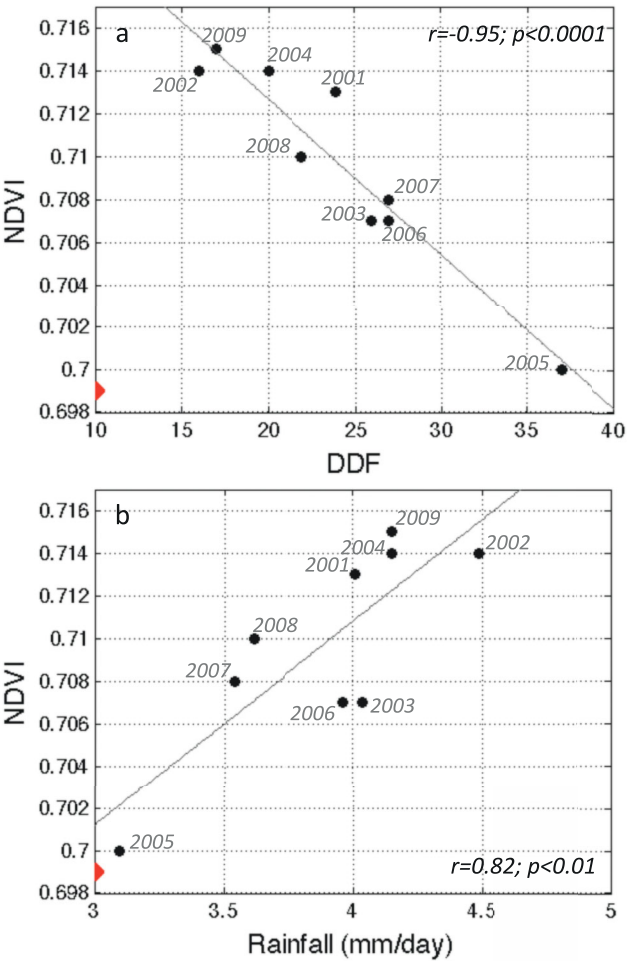


**Figure 8.** Scatterplot between annual DDF and (a) mean August–October NDVI and (b) mean April–August rainfall (mm/d) over the Tamshiyacu basin for the 2001–2009 period. Corresponding years, regression line, coefficient of correlation, and *p*-value are indicated. NVDI value for 2010 is indicated with a red triangle in the *y* axes.

the southern Amazon in recent decades [*Brienen et al.*, 2015, *Nobre et al.*, 2016]. The significant changes in DDF in the southern Tamshiyacu basin (Figure 2) and the strong relationship between DDF and NDVI indicate that the increasing number of dry days could be one of the main drivers of the decrease in greenness and carbon accumulation in the southern Amazon. It is especially important to gain a better understanding of the impact of atmospheric conditions and DDF on vegetation, because DDF is expected to increase in the future as a consequence of climate change [*Polade et al.*, 2014; *Boisier et al.*, 2015].

## 7. Summary and Final Remarks

In this study, we analyze the spatiotemporal evolution of wet-day and dry-day frequency (WDF and DDF, respectively) in the western Amazon basin, using the observed HOP rainfall data set for 1980–2009. We also investigate climatic variability related to the evolution in WDF and DDF and possible impacts of changes in rainfall intensity on vegetation in the Peruvian-Ecuadorian Amazon upstream from the Tamshiyacu station on the Amazon River.

The results suggest that WDF and DDF changed significantly in the western Amazon during 1980–2009. WDF increased after 1995, particularly over the northern part of the western Amazon (Marañón basin), while a significant increase in DDF appears over the central and southern part of this region (Ucayali basin), particularly after 1986.

The interannual evolution of WDF is positively correlated with northerly water vapor flux anomalies and negatively correlated with OLR over the northern part of Peruvian-Ecuadorian Amazon. WDF is also correlated with November–March SST in the extreme western part of the Tropical Pacific Ocean (positive correlation) and in the central Equatorial Pacific Ocean (around 150°W; negative correlation). Analysis of atmospheric circulation in a cross section of the Tropical Pacific Ocean shows that interannual variability of WDF in the western Amazon is modulated by modifications in the Walker cell during the November–March season. This mechanism enhances convective activity over the northern part of the western Amazon. Years with high WDF are associated with enhanced wind ascendance and higher-than-usual specific humidity in the western Equatorial Pacific, subsidence and weak specific humidity in the central Equatorial Pacific, and enhanced ascendance of vertical wind and higher specific humidity over the northern Peruvian-Ecuadorian Amazon basin. Our results also suggest that oceanic and atmospheric conditions that increase WDF over the western Amazon intensified after 1995, compared to the 1980–1994 period. A statistical break is detected in the WDF time series in 1995. Average annual values of WDF change from 22 days/yr before 1995 to 34 days after this date, an increase of 55%. The increase in WDF is particularly significant over the northern part of the western Amazon (the lower Marañón basin and the left bank of the Amazonas River).

The evolution of WDF explains 77% of the mean rainfall variability during the wet season (November–March) over the Peruvian-Ecuadorian Amazon, which suggests that the increased frequency of flooding after 1995 can be related to the increase of WDF over this region.

The evolution of DDF shows a significant correlation with southerly water vapor flux anomalies in the North Tropical Atlantic Ocean during the dry period (April–August). DDF variability is positively correlated with April–August SST over the North Tropical Atlantic Ocean and the Caribbean Sea. This suggests that interannual DDF variability is modulated by anomalies in the Atlantic Hadley cell during the April–August season. In fact, our results show that in years characterized by high DDF in the Tamshiyacu basin, southerly wind anomalies predominate over the western Amazon and northern South America, while enhanced wind ascendance and high specific humidity are observed over the Caribbean Sea. In contrast, a subsidence predominates over the central and southwestern Amazon, which explains the lack of rainfall and high DDF.

A significant positive trend is observed in DDF over the central and southern part of the western Amazon (Ucayali River) during 1980–2009. According to Pettitt's test, the evolution of DDF shows a break in 1986. Average annual DDF is 16.2 days/yr for 1980–1985 and 23.8 days/yr for 1986–2009. The increase in DDF is estimated at about 47%. The break in 1986 and the increase in DDF afterward is consistent with the significant change in runoff during the low-stage period at the Tamshiyacu station detected in 1986 by *Espinoza et al*. [2009b]. The evolution of DDF in the western Amazon is weakly correlated with mean rainfall during the dry season (April–August). Nonetheless, some extremely dry years (i.e., 2005) are characterized by very high DDF.

To identify possible impacts of the increase in DDF on vegetation, we compute a basin-averaged NDVI for the August–October season in the Peruvian-Ecuadorian Amazon basin as an indicator of vegetation conditions. During the 2001–2009 common period, NDVI and DDF appear significantly correlated at an interannual time scale ($r = -0.95$; $p < 0.0001$). Years characterized by high/low DDF show a significant decrease/increase in NDVI. The lowest NDVI values are observed during the extreme droughts in 2005 and 2010. The inverse association between NDVI and DDF suggests that vegetation in the western Amazon is mainly water limited, rather than light limited, and indicates that it is highly sensitive to the concentration of rainfall. The increasing DDF could therefore be one of the main drivers of the decreasing greenness of vegetation and the reduction in carbon accumulation that have been observed in the Amazon basin in recent years. These results highlight the importance of monitoring daily rainfall intensity to better evaluate the impacts of climate variability and change on Amazonian vegetation.

**Acknowledgments**

The authors acknowledge to the PNICP-Peru through the "contrato 397-PNICP-PIAP-2014" contract for funding this research. The authors are grateful to SO-HYBAM observatory for providing the HOP rainfall data available at http://www.so-hybam.org. We wish to thank the following agencies for providing access to data: the National Oceanic and Atmospheric Administration (NOAA)-Climate Prediction Center (CPC) for SST information and the National Centers for Environmental Prediction-National Center for Atmospheric Research (NCEP-NCAR) for reanalysis data (available at http://www.esrl.noaa.gov/psd/data/). We are grateful to Gérard Cochonneau, James Apaéstegui, and Barbara Fraser for their contribution to improving this paper.

## References

Aragão, L. E. O., Y. Malhi, R. M. Roman-Cuesta, S. Saatchi, L. O. Anderson, and Y. E. Shimabukuro (2007), Spatial patterns and fire response of recent Amazonian droughts, *Geophys. Res. Lett.*, *34*, L07701, doi:10.1029/2006GL028946.

Arias, P. A., R. Fu, C. Vera, and M. Rojas (2015), A correlated shortening of the North and South American monsoon seasons in the past few decades, *Clim. Dyn.*, *45*, 3183–3203, doi:10.1007/s00382-015-2533-1.

Atkinson, P. M., J. Dash, and C. Jeganathan (2011), Amazon vegetation greenness as measured by satellite sensors over the last decade, *Geophys. Res. Lett.*, *38*, L19105, doi:10.1029/2011GL049118.

Boisier, J. P., P. Ciais, A. Ducharne, and M. Guimberteau (2015), Projected strengthening of Amazonian dry season by constrained climate model simulations, *Nat. Clim. Change*, *5*(7), 656–660.

Bonal, D., B. Burban, C. Stahl, F. Wagner, and B. Hérault (2016), The response of tropical rainforests to drought—Lessons from recent research and future prospects, *Ann. For. Sci.*, *73*, 27–44, doi:10.1007/s13595-015-0522-5.

Brando, P. M., et al. (2014), Abrupt increases in Amazonian tree mortality due to drought-fire interactions, *Proc. Natl. Acad. Sci. U. S. A.*, *111*, 6347–6352, doi:10.1073/pnas.1305499111.

Brienen, R. J. W., et al. (2015), Long-term decline of the Amazon carbon sink, *Nature*, *519*, 344–348, doi:10.1038/nature14283.

Callède, J., J.-L. Guyot, J. Ronchail, Y. L'Hôte, H. Niel, and E. de Oliveira (2004), Évolution du débit de l'Amazone à Óbidos de 1902 à 1999, *Hydrol. Sci. J.*, *49*, 85–97.

Chen, J., P. Jönsson, M. Tamura, Z. Gu, B. Matsushita, and L. Eklundh (2004), A simple method for reconstructing a high-quality NDVI time-series data set based on the Savitzky–Golay filter, *Remote Sens. Environ.*, *91*(3–4), 332–344.

Chen, J. L., C. R. Wilson, and D. B. Tapley (2010), The 2009 exceptional Amazon flood and interannual terrestrial water storage change observed by GRACE, *Water Resour. Res.*, *46*, W12526, doi:10.1029/2010WR009383.

Coomes, O. T., M. Lapointe, M. Templeton, and G. List (2016), Amazon river flow regime and flood recessional agriculture: Flood stage reversals and risk of annual crop loss, *J. Hydrol.*, *539*(2016), 214–222, doi:10.1016/j.jhydrol.2016.05.027.

Davidson, E. A., et al. (2012), The Amazon basin in transition, *Nature*, *481*, 321–328, doi:10.1038/nature10717.

Debortoli, N. S., V. Dubreuil, B. Funatsu, F. Delahaye, C. Henke de Oliveira, S. Rodrigues-Filho, C. Hiroo Saito, and R. Fetter (2015), Rainfall patterns in the Southern Amazon: A chronological perspective (1971–2010), *Clim. Change*, *132*, 251–264, doi:10.1007/s10584-015-1415-1.

Espinoza, J. C., J. J. L. Ronchail Guyot, G. Cocheneau, N. Filizola, W. Lavado, E. de Oliveira, R. Pombosa, and P. Vauchel (2009a), Spatiotemporal rainfall variability in the Amazon Basin Countries (Brazil, Peru, Bolivia, Colombia and Ecuador), *Int. J. Climatol.*, *29*, 1574–1594.

Espinoza, J. C., J. L. Guyot, J. Ronchail, G. Cochonneau, N. Filizola, P. Fraizy, D. Labat, E. de Oliveira, J. Julio Ordonez, and P. Vauchel (2009b), Contrasting regional discharge evolutions in the Amazon basin (1974–2004), *J. Hydrol.*, *375*(3–4), 297–311.
Espinoza, J. C., J. Ronchail, J. L. Guyot, C. Junquas, P. Vauchel, W. Lavado, G. Drapeau, and R. Pombosa (2011), Climate variability and extreme drought in the upper Solimões River (western Amazon Basin): Understanding the exceptional 2010 drought, *Geophys. Res. Lett.*, *38*, L13406, doi:10.1029/2011GL047862.
Espinoza, J. C., M. Lengaigne, J. Ronchail, and S. Janicot (2012a), Large-scale circulation patterns and related rainfall in the Amazon Basin: A neuronal networks approach, *Clim. Dyn.*, *38*(1–2), 121–140.
Espinoza, J. C., et al. (2012b), From drought to flooding: Understanding the abrupt 2010–2011 hydrological annual cycle in the Amazonas river and tributaries, *Environ. Res. Lett.*, *7*, 024008, doi:10.1088/1748-9326/7/2/024008.
Espinoza, J. C, J. Ronchail, F. Frappart, W. Lavado, W. Santini, and J. L. Guyot (2013), The major floods in the Amazonas river and tributaries (Western Amazon basin) during the 1970–2012 period: A focus on the 2012 flood, *J. Hydrometeorol.*, *14*(3), 1000–1008.
Espinoza, J. C, J. A. Marengo, J. Ronchail, J. Molina, L. Noriega, and J. L. Guyot (2014), The extreme 2014 flood in South-Western Amazon basin: The role of tropical-subtropical South Atlantic SST gradient, *Environ. Res. Lett.*, *9*, 124007, doi:10.1088/1748-9326/9/12/124007.
Espinoza, J. C., S. Chavez, J. Ronchail, C. Junquas, K. Takahashi, and W. Lavado (2015), Rainfall hotspots over the southern tropical Andes: Spatial distribution, rainfall intensity and relations with large-scale atmospheric circulation, *Water Resour. Res.*, *51*, 3459–3475, doi: 10.1002/2014WR016273.
Fernandes, K., et al. (2011), North Tropical Atlantic influence on western Amazon fire season variability, *Geophys. Res. Lett.*, *38*, L12701, doi: 10.1029/2011GL047392.
Fernandes, K., A. Giannini, L. Verchot, W. Baethgen, and M. Pinedo-Vasquez (2015), Decadal co-variability of Atlantic SSTs and western Amazon dry-season hydroclimate in observations and CMIP5 simulations, *Geophys. Res. Lett.*, *42*, 6793–6801, doi:10.1002/2015GL063911.
Fu, R., L. Yin, W. Li, P. A. Arias, R. E. Dickinson, L. Huang, K. Fernandes, B. Liebmann, R. Fisher, and R. B. Myneni (2013), Increased dry-season length over southern Amazonia in recent decades and its implication for future climate projection, *Proc. Natl. Acad. Sci. U. S. A.*, *110*, 18,110–18,115.
Gloor, M. R. J. W., D. Brienen, T. R. Galbraith, J. Feldpausch, W. Schöngart, J. L. Guyot, J. C. Espinoza, J. Lloyd, and O. L. Phillips (2013), Intensification of the Amazon hydrological cycle over the last two decades, *Geophys. Res. Lett.*, *40*, 1729–1733, doi:10.1002/grl.50377.
Grimm, A. M., and J. P. J. Saboia (2015), Interdecadal variability of the South American precipitation in the monsoon season, *J. Clim.*, *28*(2), 755–775.
Guimberteau, M., et al. (2012), Discharge simulation in the sub-basins of the Amazon using ORCHIDEE forced by new datasets, *Hydrol. Earth Syst. Sci.*, *16*, 911–935, doi:10.5194/hess-16-911-2012.
Guimberteau, M., J. Ronchail, J. C. Espinoza, M. Lengaigne, B. Sultan, J. Polcher, G. Drapeau, J. L. Guyot, A. Ducharne, and P. Cialis (2013), Future changes in precipitation and impacts on extreme stream-flow over Amazonian sub-basins, *Environ. Res. Lett.*, *8*, 014035, doi: 10.1088/1748-9326/8/1/014035.
Hilker, T., A. I. Lyapustin, C. J. Tucker, F. G. Hall, R. B. Myneni, Y. Wang, J. Bi, Y. Mendes de Moura, and P. J. Sellers (2014), Vegetation dynamics and rainfall sensitivity of the Amazon, *PNAS*, *111*(45), 16041–16046, doi:10.1073/pnas.1404870111.
Hilker, T., A. I. Lyapustin, F. G. Hall, R. Myneni, Y. Knyazikhin, Y. Wang, C. J. Tucker, and P. J. Sellers (2015), On the measurability of change in Amazon vegetation from MODIS, *Remote Sens. Environ.*, *166*, 233–242, doi:10.1016/j.rse.2015.05.020.
Holben, B. (1986), Characteristics of maximum-value composite images from temporal AVHRR data, *Int. J. Remote Sens.*, *7*, 1417–1434.
Huete, A., K. Didan, T. Miura, E. P. Rodriguez, X. Gao, and L. G. Ferreira (2002), Overview of the radiometric and biophysical performance of the MODIS vegetation indices, *Remote Sens. Environ.*, *83*, 195–213.
Huete, A. R., K. Didan, Y. E. Shimabukuro, P. Ratana, S. R. Saleska, L. R. Hutyra, W. Yang, R. R. Nemani, and R. Myneni (2006), Amazon rainforests green-up with sunlight in dry season, *Geophys. Res. Lett.*, *33*, L06405, doi:10.1029/2005GL025583.
Jones, C., L. M. V. Carvalho, R. W. Higgins, D. E. Waliser, and J. K. E. Schemm (2004), Climatology of tropical intraseasonal convective anomalies: 1979–2002, *J. Clim.*, *17*, 523–539.
Kalnay, E., et al. (1996), The NCEP/NCAR 40-year reanalysis project, *Bull. Am. Meteorol. Soc.*, *77*, 437–71.
Kendall, M. (1975), *Rank Correlation Methods*, Grifin, London, U. K.
Lavado, W., and J. C. Espinoza (2014), Impact of El Niño and La Niña events on Rainfall in Peru, *Rev. Bras. Meteorol.*, *29*, 171–182.
Lavado, W., D. Labat, J. Ronchail, J. C. Espinoza, and J. L. Guyot (2013), Trends in rainfall and temperature in the Peruvian Amazon-Andes basin over the last 40 years (1965–2007), *Hydrol. Processes*, *41*, 2944–2957, doi:10.1002/hyp.9418.
Lee, J.-E., et al. (2013), Forest productivity and water stress in Amazonia: Observations from GOSAT chlorophyll fluorescence, *Proc. R. Soc. B*, *280*, 20130171, doi:10.1098/rspb.2013.0171.
Liebmann, B., and C. A. Smith (1996), Description of a complete (interpolated) outgoing longwave radiation dataset, *Bull. Am. Meteorol. Soc.*, *77*, 1275–1277.
Liebmann, B., G. N. Kiladis, J. A. Marengo, T. Ambrizzi, and J. D. Glick (1999), Submonthly convective variability over South America and the South Atlantic convergence zone, *J. Clim.*, *12*, 1877–1891.
Maeda, E. E., J. Heiskanen, L. E. Aragão, and J. Rinne (2014), Can MODIS EVI monitor ecosystem productivity in the Amazon rainforest?, *Geophys. Res. Lett.*, *41*, 7176–7183, doi:10.1002/2014GL061535.
Marengo, J. A., and J. C. Espinoza (2015), Review article. Extreme seasonal droughts and floods in Amazonia: Causes, trends and impacts, *Int. J. Climatol.*, *36*, 1033–1050, doi:10.1002/joc.4420.
Marengo, J. A., C. A. Nobre, J. Tomasella, M. D. Oyama, G. S. Oliveira, R. de Oliveira, H. Camargo, L. M. Alves, and I. F. Brown (2008), The drought of Amazonia in 2005, *J. Clim.*, *21*, 495–516, doi:10.1175/2007JCLI1600.1.
Marengo, J. A, J. Tomasella, L. M. Alves, W. Soares, and D. A. Rodriguez (2011), The drought of 2010 in the context of historical droughts in the Amazon region, *Geophys. Res. Lett.*, *38*, L12703, doi:10.1029/2011GL047436.
Marengo, J. A, L. M. Alves, W. R. Soares, D. A. Rodriguez, H. Camargo, M. Paredes, and A. Diaz Pablo (2013), Two contrasting seasonal extremes in tropical South America in 2012: Flood in Amazonia and drought in Northeast Brazil, *J. Clim.*, *26*(22), 9137–9154.
Morton, D. C., J. Nagol, C. C. Carabajal, J. Rosette, M. Palace, B. D. Cook, E. F. Vermote, D. J. Harding, and P. R. North (2014), Amazon forests maintain consistent canopy structure and greenness during the dry season, *Nature*, *506*(7487), 221–224.
Myneni, R. B., et al. (2007), Large seasonal swings in leaf area of Amazon rainforests, *Proc. Natl. Acad. Sci. U. S. A.*, *104*(12), 4820–4823.
Nepstad, D., P. Lefebvre, U. L. Da Silva, J. Tomasella, P. Schlesinger, L. Solorzano, P. Moutinho, D. Ray, and J. G. Benito (2004), Amazon drought and its implications for forest flammability and tree growth: A basin-wide analysis, *Global Change Biol.*, *10*(5), 704–717, doi: 10.1111/j.1529-8817.2003.00772.x.
Nobre, C. A., G. Sampaio, L. S. Borma, J. C. Castilla-Rubio, J. S. Silva, and M. Cardoso (2016), Land-use and climate change risks in the Amazon and the need of a novel sustainable development paradigm, *Proc. Natl. Acad. Sci. U. S. A.*, *113*, 10,759–10,768, doi:10.1073/pnas.1605516113.

Peixoto, J. P., and A. H. Oort (1992), *Physics of Climate*, 520 pp., Am. Inst. of Phys., New York.
Pettitt, A. (1979), A non-parametric approach to the change-point problem, *Appl. Stat.*, *28*, 126–135.
Phillips, O. L., et al. (2009), Drought sensitivity of the Amazon rainforest, *Science*, *323*, 1344–1347, doi:10.1126/science.1164033.
Polade, S. D., D. W. Pierce, D. R. Cayan, A. Gershunov, and M. D. Dettinger (2014), The key role of dry days in changing regional climate and precipitation regimes, *Nat. Sci. Rep.*, *4*, 4364, doi:10.1038/srep04364.
Reynolds, R. W., and T. M. Smith (1994), Improved global sea surface temperature analyses using optimum interpolation, *J. Clim.*, *7*, 929–948.
Ronchail, J., J.-L. Guyot, J. C. Espinoza, J. Callède, G. Cochonneau, E. DeOliveira, J. J. Ordenez, N. Filizola (2006), Impact of the Amazon tributaries on flooding in Obidos, Climate variability and Change Hydrological Impacts (Procceedings of the Fifth FRIEND World Conference), vol. 308, pp. 220–225, IAHS Publ., Havanna, Cuba.
Ropelewski, C. F., and M. A. Bell (2008), Shifts in the statistics of daily rainfall in South America conditional on ENSO phase, *J. Clim.*, *21*, 849–865.
Saatchi, S., S. Asefi-Najafabady, Y. Malhi, L. E. O. C. Aragão, L. O. Anderson, R. B. Myneni, and R. Nemani (2012), Persistent effects of severe drought on Amazonian forest canopy, *Proc. Natl. Acad. Sci. U. S. A.*, *110*, 565–570, doi:10.1073/pnas.1204651110.
Salazar, L. F., C. A. Nobre, and M. D. Oyama (2007), Climate change consequences on the biome distribution in tropical South America, *Geophys. Res. Lett.*, *34*, L09708, doi:10.1029/2007GL029695.
Saleska, S. R., K. Didan, A. R. Huete, H. R. da Rocha (2007), Amazon forests green-up during 2005 drought, *Science*, *318*(5850), 612.
Samanta, A., S. Ganguly, H. S. Hashimoto, E. Devadiga, E. Vermote, Y. Knyazikhin, R. R. Nemani, and R. B. Myneni (2010), Amazon forests did not green-up during the 2005 drought, *Geophys. Res. Lett. 37*, L05401, doi:10.1029/2009GL042154.
Satyamurty, P., C. P. W. da Costa, A. O. Manzi, and L. A. Candido (2013a), A quick look at the 2012 record flood in the Amazon Basin, *Geophys. Res. Lett.*, *40*, 1396–1401, doi:10.1002/grl.50245.
Satyamurty, P., C. P. W. da Costa, and A. O. Manzi (2013b), Moisture sources for the Amazon Basin: A study of contrasting years, *Theor. Appl. Climatol.*, *111*, 195–209, doi:10.1007/s00704-012-0637-7.
Solano, R., K. Didan, A. Jacobson, and A. Huete (2010), *MODIS Vegetation Indices (MOD13) C5 User's Guide*, Terrestrial Biophysics and Remote Sensing Laboratory, The University of Arizona, Tucson, Ariz. [Available at http://www.ctahr.hawaii.edu/grem/mod13ug/.]
Sorribas, M. V., R. C. D. Paiva, J. M. Melack, J. M. Bravo, C. Jones, L. Carvalho, E. Beighley, B. Forsberg, and M. H. Costa (2016), Projections of climate change effects on discharge and inundation in the Amazon basin, *Clim. Change*, *136*, 555–570, doi:10.1007/s10584-016-1640-2.
Villacís, M., F. Vimeux, and J. D. Taupin (2008), Analysis of the climate controls on the isotopic composition of precipitation ($\delta$18O) at Nuevo Rocafuerte, 74.5°W, 0.9°S, 250 m, Ecuador, *C. R. Geosci.*, *340*, 1–9, doi:10.1016/j.crte.2007.11.003.
Xu, L., A. Samanta, M. Costa, S. Ganguly, R. Nemani, and R. Myneni (2011), Widespread decline in greenness of Amazonian vegetation due to the 2010 drought, *Geophys. Res. Lett.*, *38*, L07402, doi:10.1029/2011GL046824.
Yin, L., R. Fu, Y.-F. Zhang, P. A. Arias, D. N. Fernando, W. Li, K. Fernandes, and A. R. Bowerman (2014), What controls the interannual variation of the wet season onsets over the Amazon?, *J. Geophys. Res. Atmos.*, *119*, 2314–2328, doi:10.1002/2013JD021349.
Yoon, J.-H., and N. Zeng (2010), An Atlantic influence on Amazon rainfall, *Clim. Dyn.*, *34*, 249–264, doi:10.1007/s00382-009-0551-6.
Zbigniew, W. (2004), Change detection in hydrological records—A review of the methodology, *Hydrol. Sci. J.*, *49*, 7–119.
Zeng, N., J. H. Yoon, J. A. Marengo, A. Subramaniam, C. A. Nobre, A. Mariotti, and D. Neelin (2008), Causes and impacts of the 2005 Amazon drought, *Environ. Res. Lett.*, *3*, 014002, doi:10.1088/1748-9326/3/1/014002.
Zou, Y., E. E. N. Macau, G. Sampaio, A. M. T. Ramos, and J. Kurths (2015), Do the recent severe droughts in the Amazonia have the same period of length?, *Clim. Dyn.*, *46*, 3279–3285, doi:10.1007/s00382-015-2768-x.

*Water Resources Research*

Supporting Information for

# Evolution of wet- and dry-day frequency in the western Amazon basin: Relationship with atmospheric circulation and impacts on vegetation

Jhan Carlo Espinoza[1*]; Hans Segura[1]; Josyane Ronchail[2]; Guillaume Drapeau[3]; Omar Gutierrez-Cori[1,4]

1.- Subdirección de Ciencias de la Atmósfera e Hidrósfera (SCAH). Instituto Geofísico del Perú (IGP), Peru
2.- Univ. Paris Diderot, Sorbonne Paris Cité, UMR Locean (Sorbonne Universités-UPMC-, CNRS, IRD, MNHN), France
3.- Université Paris Diderot, Sorbonne Paris Cité, UMR PRODIG, Paris, France
4.- Universidad Agraria La Molina, Lima, Peru.

## Contents of this file



## Introduction

This supporting information provides the Supplementary Figure S1.

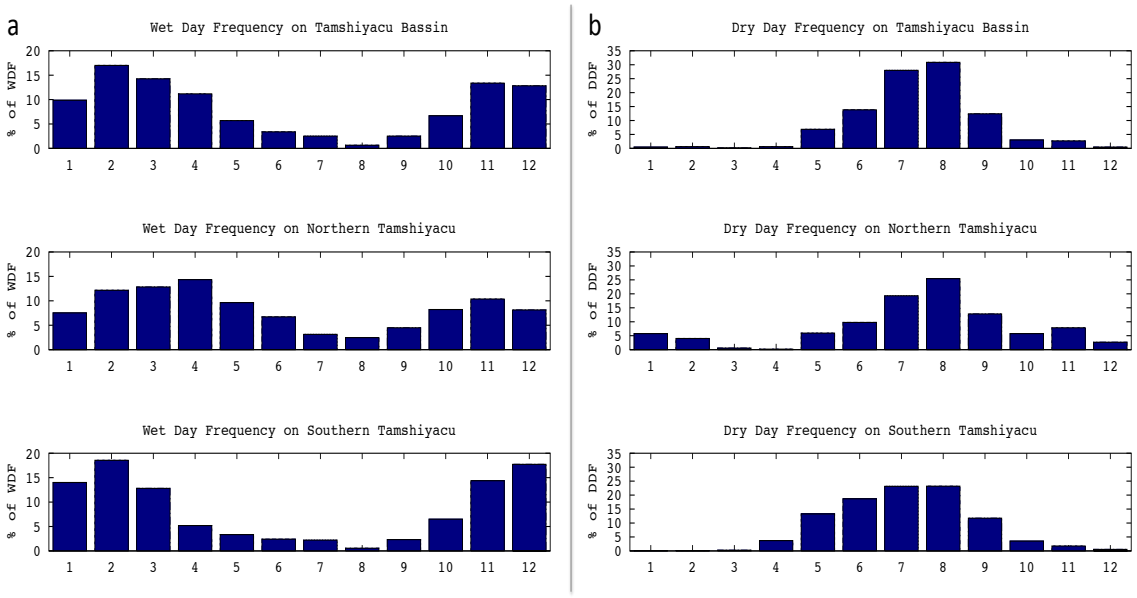


**Supplementary Figure S1.** Percentage of contribution of each month (from 1-January to 12-December) on: a) the annual wet-day frequency (WDF) and b) the annual dry-day frequency (DDF), considering (top) the whole Tamshiyacu basin, (middle) the northern part of the basin (north of 7.5°S) and (bottom) the southern part of the basin (south of 7.5°S).